**International Journal of Applied Power Engineering (IJAPE)**
Vol. 15, No. 2, June 2026, pp. 535~545
ISSN: 2252-8792, DOI: 10.11591/ijape.v15.i2.pp535-545


# Techno-economic assessment of gas engine power plants penetration in a power grid

**Adelhard Beni Rehiara[1], Frederik Haryanto Sumbung[2]**
[1]Department of Electrical Engineering, Faculty of Engineering, University of Papua, Manokwari, Indonesia
[2]Department of Electrical Engineering, Faculty of Engineering, University of Musamus, Merauke, Indonesia

**Article Info**

***Article history:***

Received Jul 20, 2025
Revised Feb 7, 2026
Accepted Mar 12, 2026

***Keywords:***

Fuel cost
Optimal power flow
Power loss minimization
Snake optimization
Voltage stability

**ABSTRACT**

This paper presents a techno-economic assessment of integrating engine power plants into a power grid, using the snake optimization (SO) algorithm to solve the multi-objective optimal power flow (OPF) problem. The study focuses on four key objectives: minimizing fuel costs, reducing voltage deviation, enhancing voltage stability, and minimizing active power losses. Simulations conducted on the 38-bus of Manokwari grid system demonstrate that the SO algorithm significantly improved performance in all areas. Fuel costs were reduced to 2.003 million USD/h while maintaining a stable voltage profile. Voltage deviation was reduced to 0.5577 p.u., ensuring better voltage consistency across the grid. Voltage stability was enhanced with a minimized $L_{max}$ value of 0.0200 p.u., and active power losses were reduced to 0.3423 MW, reflecting a notable increase in system efficiency. These findings demonstrate the effectiveness of integrating gas engine power plants, which led to noticeable improvements in operational efficiency and grid stability.



***Corresponding Author:***

Adelhard Beni Rehiara
Department of Electrical Engineering, Faculty of Engineering, University of Papua
St. Gunung Salju Amban, Manokwari 98314, Indonesia
Email: a.rehiara@unipa.ac.id

## 1. INTRODUCTION

Optimal power flow (OPF) has emerged as a fundamental optimization tool in power engineering, aimed at determining the most efficient operational conditions for electrical power systems. Since its inception in the 1960s, OPF has undergone significant evolution, addressing various challenges related to power generation and distribution [1]. The primary objective of OPF is to minimize operational costs while adhering to technical constraints such as power flow equations, voltage limits, and transmission line capacities. Its significance lies in its ability to enhance system reliability, reduce costs, and integrate renewable energy sources, contributing to the overall stability and efficiency of modern power systems [2], [3]. Various techniques, including security-constrained OPF (SCOPF), are widely adopted to maintain system security under normal and fault conditions, ensuring stable power supply across grids [4], [5].

As the complexity of power systems continues to grow, driven by increasing energy demands and the integration of distributed energy resources, advanced OPF methods are indispensable. Traditional OPF techniques often face limitations in addressing non-linear, non-convex optimization problems. Therefore, meta-heuristic algorithms such as genetic algorithms (GA), particle swarm optimization (PSO), and whale optimization algorithm (WOA) have become prominent in OPF applications. These methods are highly flexible, capable of efficiently navigating complex search spaces while avoiding local optima, offering superior solutions to power flow challenges in systems with high renewable penetration [6]-[8].

The existing literature extensively covers the application of meta-heuristic algorithms in OPF optimization, with methods such as particle swarm optimization (PSO) [9], [10], cuckoo search algorithm [11], grey wolf algorithm [12], bird swarm algorithm [13], teaching-learning-based optimization [14], [15], fire hawk optimizer [16], wolf pack algorithm [17], and elephant swarm water search [18]. These algorithms have demonstrated success in reducing power losses, improving voltage stability, and minimizing fuel costs in systems with high renewable energy integration.

Meta-heuristic methods, particularly snake optimization (SO), have shown considerable promise in solving complex optimization problems in various fields, including power engineering. Snake optimization, a nature-inspired algorithm, leverages the behavioral patterns of snakes to efficiently search for optimal solutions, demonstrating superior performance in trajectory optimization and multitask assignments [3], [19]. This method has proven effective in overcoming the limitations of traditional optimization techniques, particularly in addressing non-linear and non-convex challenges common in OPF problems [20], [21].

The SO method is a recently developed approach for addressing the OPF problem. It has demonstrated significant effectiveness in optimizing various aspects of power systems. Specifically, the method has been shown to reduce fuel costs, minimize voltage deviations, improve line stability, and decrease power losses and emissions. These results were validated through application on the standard 30-bus test system, highlighting its potential for enhancing the efficiency and reliability of electrical grids [1].

Unlike many previous OPF studies that focus primarily on renewable energy integration or standard benchmark systems, this study explicitly investigates the integration of gas engine power plants within a practical power grid. Gas engine generators are characterized by fast response, flexible dispatch capability, and distinct fuel cost characteristics, which directly influence both economic and voltage-related performance of the grid. In this work, gas engine power plants are explicitly modeled in the OPF framework using customized fuel cost functions and operational constraints. This modeling approach enables a systematic evaluation of their techno-economic impact on grid performance. A techno-economic assessment of a power grid, following the integration of gas engine power plants, is performed using SO to solve a case-based single-objective OPF problem while considering multiple performance criteria, including fuel cost, voltage deviation, voltage stability, and active power loss minimization. The main contributions of this study are threefold: i) modeling a practical power grid with gas engine power plant penetration, ii) designing appropriate fuel cost functions for gas engine generators, and iii) evaluating grid techno-economic performance using the SO-based OPF approach.

## 2. METHOD

This study employs a systematic methodology to evaluate the techno-economic performance of the Manokwari power grid after reconfiguration by solving the OPF problem using SO algorithm. The methodology consists of power system modeling, OPF formulation, implementation of the SO algorithm, and simulation parameters and setup.

### 2.1. Power system modeling and OPF formulation

The Manokwari grid was chosen for assessment due to the recent integration of two gas engine power plants into the power grid. Where the integration has altered the system configuration. The system data, including generator limits and line capacities, were obtained from [9] with some modifications due to reconfiguration by bypassing bus 1 and bus 9 with a new line having an impedance of $0.840+j1.974$ p.u., and operating two gas engine power plants connected to bus 9, each rated at 20 MW, as shown in red in Figure 1. The system assessment is done in four cases where described in objective function as follows:

Case 1: Fuel cost minimization – This case focuses on reducing the total fuel cost while ensuring that all technical constraints, such as voltage and generator limits, are respected.

Case 2: Voltage deviation improvement – The goal is to improve the voltage profile by minimizing the deviation between actual and nominal voltages.

Case 3: Voltage stability enhancement – This case aims to improve the voltage stability of the grid by minimizing the maximum voltage stability index.

Case 4: Active power loss minimization – The objective is to reduce transmission losses in the system, which contributes to increased efficiency and reduced operational costs.

The integration of gas engine power plants into the Manokwari grid is explicitly represented by modeling the gas engine units as controllable generation sources within the OPF framework. These generators are connected at designated buses and are characterized by specific active and reactive power limits, as well as quadratic fuel cost functions reflecting gas engine operational behavior. Their dispatch levels are treated as decision variables in the optimization process, allowing the SO algorithm to determine optimal operating points

under different objective scenarios. This modeling approach ensures that the impact of gas engine penetration on system economics and technical performance is directly captured in the optimization results.

The OPF problem is formulated as a constrained nonlinear optimization problem, where the objective is to determine the optimal operating point of the power system while satisfying all physical and operational constraints. The general OPF formulation is expressed as the minimization of an objective function subject to equality and inequality constraints. Equality constraints represent the power flow balance equations, ensuring that generated power meets load demand and system losses. Inequality constraints enforce generator operating limits, bus voltage limits, and transmission line flow limits.

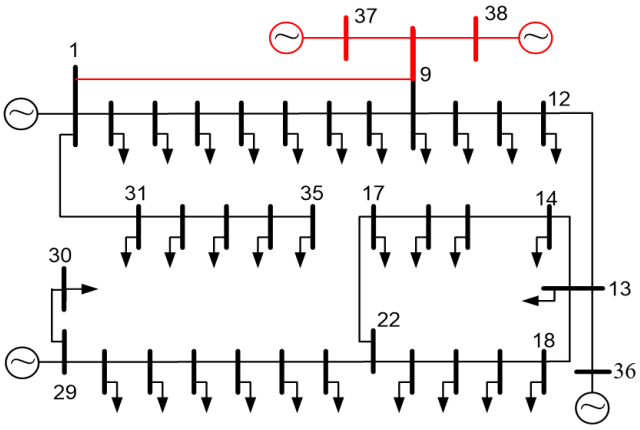


Figure 1. Single line diagram of Manokwari grid

### 2.1.1. Objective function

The objective function in OPF defines the power system's operational goal, focusing on economic efficiency, technical performance, or security. In this study, objectives reflect key economic and operational indicators for grids with gas engine power plants. Each objective is evaluated independently to assess its impact on system performance. The total objective function $J$ is to minimize or optimize the following components:

i) Fuel cost minimization: The economic objective to minimize the fuel cost of power generation is expressed as (1) [1], [9], [12], [14], [22].

$$f_1 = \sum_{i=1}^{NG}(a_i + b_i P_{Gi} + c_i P_{Gi}^2) \quad (1)$$

Where $P_{Gi}$ is the power generated by the $i$-th generator and $a_i$, $b_i$, and $c_i$ are cost coefficients.

ii) Voltage deviation minimization: To improve the voltage profile, the voltage deviation from the nominal value at the load buses is minimized using (2).

$$f_2 = \sum_{i=1}^{NG}(a_i + b_i P_{Gi} + c_i P_{Gi}^2) + 1000 \rightleftarrows \sum_{i=1}^{NL}|V_{Li} - 1| \quad (2)$$

Where $V_{Li}$ represents the voltage magnitude at load bus $i$ and $N_L$ is the number of load buses.

iii) Voltage stability enhancement: The voltage stability of the system is improved by minimizing the maximum L-index, which serves as an indicator of system stability.

$$f_3 = 6000\left(max\left(1 - \sum_{i=1}^{NG} H_{LG}\frac{V_i}{V_j}\right)\right) \quad j = 1,2,\cdots,NL \quad (3)$$

Where $H_{LG}$ is the submatrix of the bus admittance matrix and $V_i$, $V_j$ are the voltage magnitudes at buses $i$ and $j$, respectively.

iv) Active power loss minimization: The total active power loss in the transmission system is minimized.

$$f_4 = \sum_{k=1}^{NL} G_k\left(V_i^2 + V_j^2 - 2V_iV_j\,cos\left(\delta_i - \delta_j\right)\right) \quad (4)$$

Where $G_k$ is the conductance of branch $k$ and $\delta_i$, $\delta_j$ are the voltage angles at buses $i$ and $j$.

#### 2.1.2. Equality and inequality constraints

The OPF problem must satisfy equality and inequality constraints representing physical and operational limits of the power system. These constraints ensure balanced power generation and consumption, acceptable system voltages, and safe transmission line operation. Standard power flow equations and operating limits are adopted to model real-world system conditions accurately.

i) Power flow equations (equality constraints): The power balance equations for active and reactive power at each bus must be satisfied [1], [9], [12], [14], [22].

$$P_{Gi} - P_{Di} = \sum_{i=1}\left(V_i V_j Y_{ij}\, cos\left(\theta_{ij} + \delta_i - \delta_j\right)\right) \quad (5)$$

$$Q_{Gi} - Q_{Di} = \sum_{i=1}\left(V_i V_j Y_{ij}\, sin\left(\theta_{ij} + \delta_i - \delta_j\right)\right) \quad (6)$$

Where $P_{Gi}$, $Q_{Gi}$, $P_{Di}$, and $Q_{Di}$ represent the active and reactive power generation and demand at bus $i$, and $Y_{ij}$ and $\theta_{ij}$ are the magnitude and angle of the admittance matrix between buses $i$ and $j$.

ii) System operating constraints (inequality constraints): These include limits on generator output, bus voltage, and transmission line capacity [1], [9], [12], [14], [22].

$$P_{Gi}^{min_{Gi}}{}_{Gi}^{max_G} \quad (7)$$

$$Q_{Gi}^{min_{Gi}}{}_{Gi}^{max_G} \quad (8)$$

$$V_{Gi}^{min_{Gi}}{}_{Gi}^{max_G} \quad (9)$$

$$V_i^{min_i}{}_i^{max} \quad (10)$$

$$S_{ij} \leq S_{ij}^{max} \quad (11)$$

Where $P_{Gi}^{\min}$ and $P_{Gi}^{\max}$ are the minimum and maximum generation limits, $V_{Gi}^{\min}$ and $V_{Gi}^{\max}$ are the voltage limits, and $S_{ij}^{\max}$ is the thermal limit of the transmission line between buses $i$ and $j$.

### 2.2. Snake optimization algorithm for OPF

To solve the formulated OPF problem, the SO algorithm is employed. SO is a population-based metaheuristic inspired by the natural behaviors of snakes, such as food searching, competition, and mating. These behaviors are mathematically modeled to balance exploration and exploitation during the search process, making SO suitable for solving nonlinear and non-convex optimization problems such as OPF.

In the SO-based OPF implementation, each candidate solution (snake) represents a complete set of OPF control variables, including generator active power outputs, generator voltage magnitudes, transformer tap settings, and shunt reactive power compensations. The optimization process begins by randomly initializing a population of snakes within the feasible bounds of the control variables. The population is then divided into male and female groups, and the fitness of each snake is evaluated using the selected OPF objective function. The procedure of SO-based OPF is done under some steps as follows [23]-[27].

i) Step 1: Initialization

The optimization process starts by randomly generating an initial population of snakes within the allowable bounds of the OPF control variables using (12), under upper ($Ub$) and lower bound ($Lb$). The total population is then equally divided into male and female groups. Each snake is evaluated using the OPF objective function to determine its fitness.

$$x_i = Lb + r(Ub - Lb) \quad (12)$$

ii) Step 2: Fitness evaluation

The best-performing snakes in the male ($f_{best,m}$) and female ($f_{best,f}$) are identified. Two key parameters—food quantity ($Q_F$) and temperature ($T_A$)—are computed using (13) and (14). These parameters govern the behavioral state of the snake population and determine the subsequent search strategy.

$$T_A = exp\left(-t/t_{max}\ ()\right) \quad (13)$$

$$Q_F = 0.5\ \ exp\left(t - t_{max}/t_{max}\right) \quad (14)$$

iii) Step 3: Exploration mode (QF < 0.25)

When the food quantity is low, the algorithm enters the exploration phase. In this phase, snake positions are updated using (15) and (16) to encourage wide exploration of the search space. This step enhances global search capability and helps avoid local optima. The food acquisition abilities of male and female ($A_m$ and $A_f$), snakes, defined in (17) and (18), regulate the exploration process.

$$X_{i,m}(t+1) = X_{r,m}(t) \pm 0.05A_m((Ub - Lb)rand(Lb)) \quad (15)$$

$$X_{i,f}(t+1) = X_{r,f}(t) \pm 0.05A_f((Ub - Lb)rand(Lb)) \quad (16)$$

$$A_m = exp\left(-f_{r,m}/f_{i,m}\right) \quad (17)$$

$$A_f = exp\left(-f_{r,f}/f_{i,f}\right) \quad (18)$$

iv) Step 4: Exploitation mode ($Q_F \geq 0.25$ and $T_A > 0.6$)

If sufficient food is available and the temperature is high, the algorithm switches to exploitation mode. In this mode, snakes update their positions using (19), focusing on refining solutions around the current best candidates to improve convergence accuracy.

$$X_{i,j}(t+1) = X_{food} \pm 2T_A rand(X_{food} - X_{i,j}(t) \quad (19)$$

v) Step 5: Mating or fighting mode ($Q_F \geq 0.25$ and $T_A \leq 0.6$)

When the temperature is low, the algorithm probabilistically selects either mating or fighting behavior. In the mating mode ($F_m$ and $F_f$), new offspring solutions are generated using (20) and (21), with fighting abilities ($M_m$ and $M_f$) defined in (22) and (23). If fighting mode is selected, snake positions are updated using (24) and (25), while mating abilities are calculated using (26) and (27). These behaviors maintain population diversity and balance exploration and exploitation.

$$X_{i,m}(t+1) = X_{i,m}(t) + 2F_M rand(Q_F(X_{best,f} - X_{i,m}(t) \quad (20)$$

$$X_{i,f}(t+1) = X_{i,f}(t) + 2F_F rand(Q_F(X_{best,m} - X_{i,f}(t) \quad (21)$$

$$F_m = exp\left(-f_{best,m}/f_i\right) \quad (22)$$

$$F_f = exp\left(-f_{best,f}/f_i\right) \quad (23)$$

$$X_{i,m}(t+1) = X_{i,m}(t) + 2M_m rand(Q_F(X_{i,f}(t) - X_{i,m}(t)) \quad (24)$$

$$X_{i,f}(t+1) = X_{i,f}(t) + 2M_f rand(Q_F(X_{i,m}(t) - X_{i,f}(t)) \quad (25)$$

$$M_m = exp\left(-f_{i,f}/f_{i,m}\right) \quad (26)$$

$$M_f = exp\left(-f_{i,m}/f_{i,f}\right) \quad (27)$$

vi) Step 6: Replacement (egg-hatching mechanism)

After the behavioral updates, weak snakes are identified and replaced with newly generated offspring using (28) and (29). This replacement mechanism prevents premature convergence and ensures sustained diversity within the population.

$$X_{worst,m} = Lb + rand(Ub - Lb) \quad (28)$$

$$X_{worst,f} = Lb + rand(Ub - Lb) \quad (29)$$

vii) Step 7: Termination and output

Steps 2–6 are repeated until the termination criterion is satisfied, such as reaching the maximum number of iterations or achieving convergence. The overall procedure of the snake optimization algorithm applied to the OPF problem summarizes the sequence of initialization, fitness evaluation, behavioral mode selection, solution updating, replacement, and termination. The best solution obtained at the end of the process represents the optimal OPF solution for the selected objective.

### 2.3. Simulation parameters and setup

The simulations for this study were conducted using the Matpower 7.0 software package, speeding the OPF computation. The software was run on an Intel Core i7-2677M CPU with 10 GB of RAM, under a Windows 10 operating system. This environment was sufficient to handle the computational demands of the simulation, providing timely results while ensuring data integrity.

A population size of 50 was selected for the algorithm, balancing computational efficiency with solution accuracy. A maximum of 100 iterations was used to ensure that the algorithm had enough time to converge to an optimal solution while avoiding unnecessary computational overhead. This combination of parameters was designed to strike a balance between the exploration and exploitation phases of the SO algorithm, ensuring that the solutions found were both globally optimal and computationally efficient.

## 3. RESULTS AND DISCUSSION

### 3.1. Design fuel cost function

In the context of OPF problems, the fuel cost function plays a crucial role as the primary objective to be minimized, ensuring that economic efficiency is achieved while satisfying the technical constraints of the power grid. The process of designing a fuel cost function for gas engine power plants involves creating a mathematical model that accurately represents the operational costs associated with power generation. With the operation of the two gas engine power plants in the grid of Manokwari, it is essential to formulate the fuel cost function of the power plants. Based on the provided data in [28]. the cost functions can be determined using a simple quadratic equation that accounts for the power output and fuel consumption characteristics of the plants, as follows:

$$F_{37} = 1082.5\text{-}0.0627P_{37} + 1e^{-5}P_{37}^2$$
$$F_{38} = 2059.5\text{-}0.3264P_{38} + 3e^{-5}P_{38}^2$$

### 3.2. Fuel cost minimization

The goal in Case 1 was to minimize fuel costs while maintaining acceptable system performance. According to Table 1, the total fuel cost for this case was approximately 2.003 million USD/h. This result shows a significant reduction in operating costs, driven by optimal control over active power generation values $P_1$ to $P_{38}$, where minimal adjustments to power outputs were applied. In this case, P1 remained near zero, while $P_{37}$ and $P_{38}$ were significantly higher, reflecting the efficient use of different generation units to keep costs low. This achievement is validated in [9], where the other power plants work at maximum while the rest will be handled by $P_1$.

Regarding the voltage profile in Figure 2, Case 1 resulted in relatively stable voltages across all buses, with most buses showing values near or slightly above 1.0 per unit (p.u.). The highest deviation from the nominal value was observed at bus 30, with a voltage of 0.9885 p.u., which indicates that while cost minimization was achieved, some minor voltage drops occurred, especially at the lower-end buses. However, these values remained within acceptable operating limits, ensuring the system's reliability and security. The loss of active power in this scenario was relatively high, at 10.333 MW. This loss is a trade-off often encountered in cost-minimization strategies, where the system's configuration may prioritize lower costs over minimal power losses. However, the focus on fuel cost minimization ensures that the financial benefits outweigh the small increase in power losses and the voltage deviation observed in some parts of the system.

Table 1. Variables change in each case

| Variable | Case 1 | Case 2 | Case 3 | Case 4 |
|---|---|---|---|---|
| $P_1$ (MW) | 0.0001 | 6.0660 | 19.2410 | 22.8740 |
| $P_{29}$ (MW) | 0.2500 | 2.3803 | 2.3549 | 2.5000 |
| $P_{36}$ (MW) | 2.0000 | 19.0420 | 6.5678 | 2.0000 |
| $P_{37}$ (MW) | 20.0000 | 19.0420 | 2.0000 | 2.0000 |
| $P_{38}$ (MW) | 19.1148 | 19.0420 | 2.0000 | 2.0000 |
| $Q_1$ (MVar) | 41.6950 | 56.7000 | 19.2310 | 16.3340 |
| $Q_{29}$ (MVar) | 5.8883 | 1.4309 | 2.5000 | 2.4211 |
| $Q_{36}$ (MVar) | - 0.3454 | - 4.8304 | - 2.7902 | - 0.7413 |
| $Q_{37}$ (MVar) | - 8.7631 | - 3.3273 | - 1.0564 | - 1.2470 |
| $Q_{38}$ (MVar) | - 8.2702 | - 3.3273 | - 1.0564 | - 1.2470 |
| Cost (milion USD/h) | 2.0033 | 2.1497 | 2.7088 | 2.9213 |
| Ploss (MW) | 10.3330 | 22.4080 | 1.1316 | 0.3423 |
| VD (p.u.) | 0.9193 | 0.5577 | 1.1755 | 1.1604 |
| L-max (p.u.) | 0.0273 | 0.0535 | 0.0200 | 0.0288 |

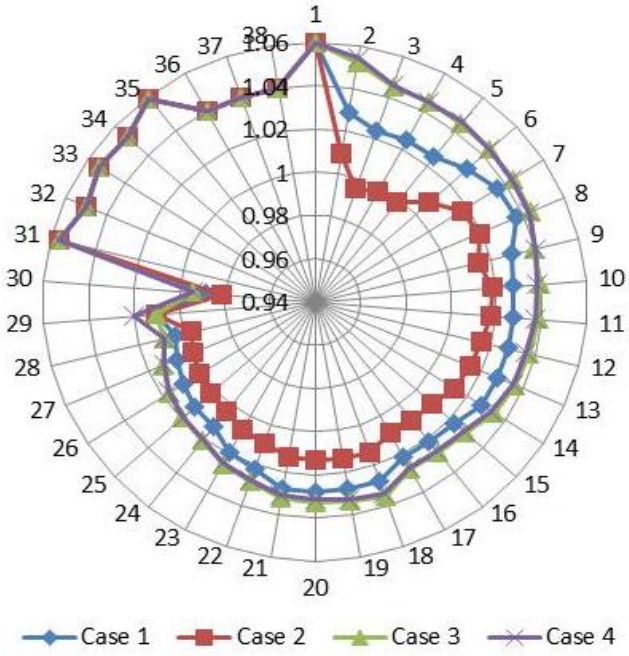


Figure 2. Voltage profile in each case

### 3.3. Voltage deviation improvement

In Case 2, the primary focus was on improving the voltage deviation (VD) across the network. According to Table 1, this strategy yielded the lowest VD value of 0.5577 p.u., a significant improvement over Case 1's 0.9193 p.u. The optimization in this case resulted in much more uniform voltage profiles across all buses, as seen in Figure 2. The largest deviation from 1.0 p.u. occurred at bus 30, where the voltage dropped to 0.98156 p.u., but overall, the system maintained a more balanced voltage distribution.

However, the improvements in voltage profiles came at a higher operational cost. The total fuel cost increased to 2.1497 million USD/h, which reflects the additional efforts in adjusting generator outputs to enhance voltage profiles. In this case, the power outputs $P_1$ to $P_{38}$ show significant variation, especially in $P_1$, which increased from nearly zero in Case 1 to 6.0659 MW. This indicates that the system had to utilize different generation sources and operate them at higher outputs to achieve the desired voltage improvement. Furthermore, the active power losses in this case increased dramatically to 22.408 MW, indicating that the system had to endure higher losses to maintain the voltage profile improvement. This trade-off highlights the balance between improving voltage stability and managing system efficiency, where voltage improvements often come at the cost of higher active power losses and increased operating expenses. The result is the same as in [1], [14], [22], where the VD is lower, the fuel cost is reduced, and the power loss is higher.

### 3.4. Voltage stability enhancement

Voltage stability enhancement was the key objective in Case 3, where the system aimed to improve long-term voltage stability across all buses. According to Table 1, the $L_{max}$ index, which represents the maximum loadability limit, was reduced to 0.0200 p.u., the lowest among all cases, indicating a notable improvement in voltage stability. This lower $L_{max}$ means that the system could handle more load without facing instability, a critical factor for preventing voltage collapse under stressed conditions.

In terms of the voltage profile, given in Figure 2, Case 3 maintained relatively high voltage levels across the network, with most buses having voltages close to 1.05 p.u. The only notable dip occurred at bus 30, where the voltage reached 0.99423 p.u., still within acceptable bounds. This result suggests that voltage stability was achieved without causing significant deviations, which is a positive outcome compared to other cases. This finding is validated in [1], [9], [12], where voltage deviation is increased when $L_{max}$ is lower.

The focus on voltage stability came at a higher cost of 2.7088 million USD/h and increased power losses (1.1316 MW) compared to Case 1 but lower than Case 2. This indicates that while the system prioritized long-term voltage stability, it still managed to maintain reasonable power loss levels, balancing stability and efficiency effectively. The improvement in stability is crucial for system reliability, especially under varying load conditions.

### 3.5. Active power loss depreciation

Reducing losses is crucial for improving the overall efficiency of the power grid and ensuring that more of the generated power reaches consumers. In Case 4, the system aimed to minimize active power losses. This effort led to the lowest power loss among all cases, with a value of 0.3423 MW, as indicated in Table 1. By minimizing these losses, the system improved overall efficiency, reducing waste in energy transmission. This achievement reflects the effectiveness of optimized dispatch strategies, particularly in the adjustments made to the power outputs $P_1$ to $P_{38}$, which were kept relatively low, except for $P_1$ at 22.874 MW. Since $P_1$ is close to the load bus of bus 31-35, the output of the other power plant behind the reactance might be minimized as same in [9].

The voltage profile in Case 4, presented in Figure 2, shows a stable system with minimal voltage deviation. Most buses maintained a voltage close to 1.04 p.u., except for a slight drop at bus 30 (0.9942 p.u.). These results indicate that power loss minimization did not come at the expense of voltage stability, showcasing the efficiency of the system in managing both objectives simultaneously. However, this improvement in power loss reduction came at the highest operational cost, reaching 2.9213 million USD/h. This reflects the typical trade-off where minimizing losses often requires higher investment in resources and control mechanisms. While the cost was substantial, the benefit of reducing energy waste can justify the expense, especially in systems where power losses represent a significant operational challenge.

### 3.6. Assessment summary

Each of the four cases presented different trade-offs between cost, voltage stability, voltage deviation, and power losses. In Case 1, the focus was on minimizing fuel costs, resulting in relatively stable voltage profiles but higher power losses. Case 2 aimed to improve voltage deviation, achieving better voltage uniformity at the expense of higher costs and power losses. Case 3 emphasized voltage stability, leading to improved system reliability, though with a moderate increase in costs and power losses. Case 4, focused on minimizing active power losses, achieved the best performance in terms of efficiency but incurred the highest operational costs. The voltage profile remained stable and the system was able to minimize losses.

Each case demonstrates a unique approach to optimizing different aspects of power system performance, highlighting the balance between operational costs, system reliability, and efficiency. However, the results show that there is no one-size-fits-all solution, and each optimization goal has its benefits and drawbacks. Depending on the priorities of a power system, operators can choose the appropriate strategy to minimize costs, improve voltage performance, or reduce losses, keeping in mind the associated trade-offs. From a system-level perspective, the results indicate that the inclusion of gas engine power plants plays a significant role in enhancing grid flexibility and operational performance. Compared to traditional generation dispatch, gas engine units provide effective support for voltage regulation and loss reduction due to their proximity to load centers and adjustable output capability. The relative performance improvements observed across the four cases highlight that gas engine penetration, when optimally dispatched using the SO-based OPF approach, contributes not only to economic benefits but also to improved voltage stability and transmission efficiency.

In addition to absolute performance evaluation, a relative analysis is performed to contextualize the effectiveness of the proposed snake optimization (SO)-based OPF approach. Across the four cases, the SO algorithm demonstrates a consistent trade-off between economic and technical objectives. Case 2 achieves a 39.3% reduction in voltage deviation compared to Case 1, at the expense of increased fuel cost and power

losses. Case 3 further improves voltage stability by approximately 62.6% relative to Case 2 with moderate cost increases. Moreover, Case 4 attains a 96.7% reduction in active power losses compared to Case 1, highlighting the strong capability of SO in loss minimization.

From a methodological perspective, the results are competitive with other meta-heuristic-based OPF approaches, such as PSO, grey wolf optimizer, and teaching–learning-based optimization [12], [15], [17], [22]. Although direct numerical comparison is constrained by differences in system configurations and objectives, the achieved fuel cost, voltage stability, and loss reduction are comparable to or better than those reported in the literature. This confirms the robustness and practical applicability of the proposed SO-based OPF framework for power systems with gas engine power plant integration.

## 4. CONCLUSION

This paper presents a comprehensive techno-economic assessment of the Manokwari power grid following the integration of gas engine power plants, utilizing the OPF framework. The SO algorithm was applied to solve the multi-objective OPF problem, resulting in significant improvements across key performance metrics. The assessment focused on four critical objectives: minimizing fuel costs, reducing voltage deviation, enhancing voltage stability, and minimizing active power losses. The implementation of the SO algorithm demonstrated its effectiveness in optimizing the grid's operational efficiency while addressing both economic and technical challenges posed by the integration of gas engine power plants.

The results of the assessment clearly demonstrate the significant impact of gas engine power plant penetration on the performance of the Manokwari power grid. The integration of these power plants led to noticeable improvements in operational efficiency and grid stability. Fuel cost minimization, achieved through the SO algorithm, reduced costs to 2.003 million USD/h, indicating that the penetration of gas engine power plants contributed to more economical power generation. Furthermore, the voltage deviation across the grid was substantially reduced, improving voltage consistency and reducing the overall stress on the grid, a direct result of the enhanced system configuration following the plant integration.

The assessment also revealed that the penetration of gas engine power plants had a positive impact on voltage stability, with the maximum $L_{max}$ index decreasing to 0.0200 p.u., thereby ensuring stronger grid stability under varying load conditions. Additionally, active power losses were minimized to 0.3423 MW, reflecting the increased efficiency brought about by the power plant integration. These findings highlight the crucial role that the introduction of gas engine power plants plays in optimizing grid performance, demonstrating that such integration not only enhances economic outcomes but also significantly improves the technical stability and efficiency of the power system. Overall, the study confirms that gas engine power plants, when properly integrated and optimized, act as flexible and economically efficient generation resources that significantly enhance both the technical and economic performance of practical power grid systems.

Future research may extend this work by incorporating renewable energy sources, such as solar and wind power, alongside gas engine power plants to evaluate system performance under higher levels of generation variability. In addition, uncertainty modeling related to load demand, fuel price fluctuations, and renewable intermittency could be integrated to better reflect real-world operating conditions. Further extensions may consider comparative studies with other advanced meta-heuristic algorithms or the application of the proposed approach to dynamic or security-constrained OPF formulations for practical smart grid deployment.

## ACKNOWLEDGMENTS

The authors would like to express their gratitude to their colleagues in the Electrical Engineering Departments at both the University of Papua and the University of Musamus for their valuable insights and expertise, which significantly contributed to the success of this research.

## FUNDING INFORMATION

Authors state no funding involved.

## AUTHOR CONTRIBUTIONS STATEMENT

This journal uses the Contributor Roles Taxonomy (CRediT) to recognize individual author contributions, reduce authorship disputes, and facilitate collaboration.

| Name of Author | C | M | So | Va | Fo | I | R | D | O | E | Vi | Su | P | Fu |
|---|---|---|---|---|---|---|---|---|---|---|---|---|---|---|
| Adelhard Beni Rehiara | ✓ | ✓ | ✓ | ✓ | ✓ | ✓ | ✓ | ✓ | ✓ | ✓ | | ✓ | ✓ | |
| Frederik Haryanto Sumbung | | ✓ | | | | ✓ | | ✓ | ✓ | ✓ | ✓ | | | ✓ |

C : **C**onceptualization
M : **M**ethodology
So : **So**ftware
Va : **Va**lidation
Fo : **Fo**rmal analysis
I : **I**nvestigation
R : **R**esources
D : **D**ata Curation
O : Writing - **O**riginal Draft
E : Writing - Review & **E**diting
Vi : **Vi**sualization
Su : **Su**pervision
P : **P**roject administration
Fu : **Fu**nding acquisition

## CONFLICT OF INTEREST STATEMENT

Authors state no conflict of interest.

## DATA AVAILABILITY

Data availability is not applicable to this paper as no new data were created in this study.

## REFERENCES


[1] A. B. Rehiara, E. K. Bawan, A. D. Palintin, B. R. Wihyawari, F. Y. S. Paisey, and Y. R. Pasalli, "Snake optimization based optimal power flow," *International Journal of Intelligent Engineering and Systems*, vol. 17, no. 5, pp. 683–693, Oct. 2024, doi: 10.22266/ijies2024.1031.52.

[2] K. Rajalashmi and S. U. Prabha, "Investigation of multi-objective optimal power flow problem in power system," *i-manager's Journal on Power Systems Engineering*, vol. 3, no. 1, pp. 23–28, Apr. 2015, doi: 10.26634/jps.3.1.3356.

[3] E. H. Houssein, M. H. Hassan, M. A. Mahdy, and S. Kamel, "Development and application of equilibrium optimizer for optimal power flow calculation of power system," *Applied Intelligence*, vol. 53, no. 6, pp. 7232–7253, Mar. 2023, doi: 10.1007/s10489-022-03796-7.

[4] C. Fu, Y. Zhong, P. Zhang, X. He, Y. Yang, and J. Zuo, "VSC-HVDC incorporated corrective security-constrained optimal power Flow," *Journal of Physics: Conference Series*, vol. 2320, no. 1, p. 012006, Aug. 2022, doi: 10.1088/1742-6596/2320/1/012006.

[5] A. Khan, H. Hizam, N. I. Abdul-Wahab, and M. L. Othman, "Solution of optimal power flow using non-dominated sorting multi objective based hybrid firefly and particle swarm optimization algorithm," *Energies*, vol. 13, no. 16, p. 4265, Aug. 2020, doi: 10.3390/en13164265.

[6] A. A. El-Fergany and H. M. Hasanien, "Single and multi-objective optimal power flow using grey wolf optimizer and differential evolution algorithms," *Electric Power Components and Systems*, vol. 43, no. 13, pp. 1548–1559, Aug. 2015, doi: 10.1080/15325008.2015.1041625.

[7] M. Sedighizadeh, A. Rezazadeh, and M. S. Yazdi, "Pricing of reactive power service in deregulated electricity markets based on particle swarm optimization," *International Journal of Computer and Electrical Engineering*, pp. 960–963, 2010, doi: 10.7763/IJCEE.2010.V2.259.

[8] N. B. Saputra, M. Putri, and Cholish, "A comparison of active power generated under normal circumstances with the optimization state electric power system," *International Journal of Research and Review*, vol. 10, no. 3, pp. 584–590, Mar. 2023, doi: 10.52403/ijrr.20230365.

[9] A. B. Rehiara, "Optimal power flow of the Manokwari power grid regarding penetration of 20 MW combined cycle power plant," in *2019 International Conference on Advanced Mechatronics, Intelligent Manufacture and Industrial Automation (ICAMIMIA)*, Oct. 2019, pp. 53–57, doi: 10.1109/ICAMIMIA47173.2019.9223393.

[10] S. A. Mohamed, N. Anwer, and M. M. Mahmoud, "Solving optimal power flow problem for IEEE-30 bus system using a developed particle swarm optimization method: towards fuel cost minimization," *International Journal of Modelling and Simulation*, vol. 45, no. 1, pp. 307–320, Jan. 2025, doi: 10.1080/02286203.2023.2201043.

[11] T. R. Nartu, M. S. Matta, S. Koratana, and R. K. Bodda, "A fuzzified Pareto multiobjective cuckoo search algorithm for power losses minimization incorporating SVC," *Soft Computing*, vol. 23, no. 21, pp. 10811–10820, Nov. 2019, doi: 10.1007/s00500-018-3634-7.

[12] S. Haddi, O. Bouketir, and T. Bouktir, "Improved optimal power flow for a power system incorporating wind power generation by using grey wolf optimizer algorithm," *Advances in Electrical and Electronic Engineering*, vol. 16, no. 4, Dec. 2018, doi: 10.15598/aeee.v16i4.2883.

[13] K. Aurangzeb, S. Shafiq, M. Alhussein, Pamir, N. Javaid, and M. Imran, "An effective solution to the optimal power flow problem using meta-heuristic algorithms," *Frontiers in Energy Research*, vol. 11, Sep. 2023, doi: 10.3389/fenrg.2023.1170570.

[14] H. R. E. H. Bouchekara, M. A. Abido, and M. Boucherma, "Optimal power flow using teaching-learning-based optimization technique," *Electric Power Systems Research*, vol. 114, pp. 49–59, Sep. 2014, doi: 10.1016/j.epsr.2014.03.032.

[15] M. Ahmadipour, M. M. Othman, R. Bo, M. S. Javadi, H. M. Ridha, and M. Alrifaey, "Optimal power flow using a hybridization algorithm of arithmetic optimization and aquila optimizer," *Expert Systems with Applications*, vol. 235, p. 121212, Jan. 2024, doi: 10.1016/j.eswa.2023.121212.

[16] W. N. A.-D. Abed, "Solving probabilistic optimal power flow with renewable energy sources in distribution networks using fire hawk optimizer," *e-Prime - Advances in Electrical Engineering, Electronics and Energy*, vol. 6, p. 100370, Dec. 2023, doi: 10.1016/j.prime.2023.100370.

[17] H. M. Zhuang and X. J. Jiang, "A wolf pack algorithm for active and reactive power coordinated optimization in active distribution network," *IOP Conference Series: Earth and Environmental Science*, vol. 40, p. 012003, Aug. 2016, doi: 10.1088/1755-1315/40/1/012003.

[18] O. D. Montoya, W. Gil-González, and M. Holguín, "Optimal power flow studies in direct current grids: an application of the bio-inspired elephant swarm water search algorithm," *Journal of Physics: Conference Series*, vol. 1403, no. 1, p. 012010, Nov. 2019, doi: 10.1088/1742-6596/1403/1/012010.
[19] E. S. Maputi and R. Arora, "Multi-objective optimization of a 2-stage spur gearbox using NSGA-II and decision-making methods," *Journal of the Brazilian Society of Mechanical Sciences and Engineering*, vol. 42, no. 9, p. 477, Sep. 2020, doi: 10.1007/s40430-020-02557-2.
[20] S. Masrom, A. S. A. Rahman, S. Z. Z. Abidin, N. Omar, and Z. I. Rizman, "The implementation frameworks of meta-heuristics hybridization with dynamic parameterization," *Journal of Fundamental and Applied Sciences*, vol. 9, no. 6S, p. 558, Feb. 2018, doi: 10.4314/jfas.v9i6s.41.
[21] R. S. Rao and V. S. Rao, "A generalized approach for determination of optimal location and performance analysis of FACTs devices," *International Journal of Electrical Power & Energy Systems*, vol. 73, pp. 711–724, Dec. 2015, doi: 10.1016/j.ijepes.2015.06.004.
[22] W. Warid, H. Hizam, N. Mariun, and N. Abdul-Wahab, "Optimal power flow using the jaya algorithm," *Energies*, vol. 9, no. 9, p. 678, Aug. 2016, doi: 10.3390/en9090678.
[23] F. A. Hashim and A. G. Hussien, "Snake optimizer: a novel meta-heuristic optimization algorithm," *Knowledge-Based Systems*, vol. 242, p. 108320, Apr. 2022, doi: 10.1016/j.knosys.2022.108320.
[24] F. Belabbes, D. T. Cotfas, P. A. Cotfas, and M. Medles, "Using the snake optimization metaheuristic algorithms to extract the photovoltaic cells parameters," *Energy Conversion and Management*, vol. 292, p. 117373, Sep. 2023, doi: 10.1016/j.enconman.2023.117373.
[25] W. Zheng, S. Pang, N. Liu, Q. Chai, and L. Xu, "A compact snake optimization algorithm in the application of WKNN fingerprint localization," *Sensors*, vol. 23, no. 14, p. 6282, Jul. 2023, doi: 10.3390/s23146282.
[26] Z. Li, Z. Cheng, and Y. Wang, "Parameter tuning of active disturbance rejection control based on improved snake optimization algorithm," in *2022 International Conference on Artificial Intelligence, Information Processing and Cloud Computing (AIIPCC)*, Aug. 2022, pp. 316–322, doi: 10.1109/AIIPCC57291.2022.00074.
[27] C. Yan and N. Razmjooy, "Optimal lung cancer detection based on CNN optimized and improved snake optimization algorithm," *Biomedical Signal Processing and Control*, vol. 86, p. 105319, Sep. 2023, doi: 10.1016/j.bspc.2023.105319.
[28] K. Arnold, "Analysis of the influence of load changes on fuel consumption of power plants (case study of the 20 MW Manokwari PLTMG)," Thesis, University of Papua, Manokwari, 2023.

## BIOGRAPHIES OF AUTHORS

**Adelhard Beni Rehiara** received the B.Eng. in electrical engineering from Widya Gama University, Malang, Indonesia, in 1999 and the M.S. degree in control systems engineering from HAN University, Netherlands, in 2008. He gains the Ph.D. degree in system cybernetics from Hiroshima University, Japan, in 2019. Since 2024, he has been a professor with the Electrical Engineering Department, University of Papua, Manokwari, Indonesia. He is a member of IEEE and the Institution of Engineers Indonesia (PII). His research interest includes power system optimization, power electronics, control system and machine learning. He can be contacted at email: a.rehiara@unipa.ac.id.

**Frederik Haryanto Sumbung** is an assistant professor at the Department of Electrical Engineering, University of Musamus, Merauke, Indonesia, where he has been a faculty member since 2001. He graduated a Bachelor of Engineering (B.Eng.) in electrical engineering from Universitas Kristen Indonesia Paulus, Indonesia, in 1999, and a Master of Engineering (M.Eng.) in electrical engineering from Gadjah Mada University, Indonesia, in 2008. He can be contacted at email: frederik@unmus.ac.id.